energies

MDPI

Article

Increasing Safety in an Underground Coal Mine through Degasification by Vertical Wells—Influence of the Relationship between the Permeability of Carbon and the Filter Cake of the Bentonite Suspension

Susana Torno * and Javier Toraño

Mining and Civil Works Research Group, School of Mines, Oviedo University, Independencia 13, 33005 Oviedo, Asturias, Spain; jta@uniovi.es

* Correspondence: tornosusana@uniovi.es; Tel.: +34-985-104-254; Fax: +34-985-104-245

Abstract: The Hullera Vasco Leonesa (HVL) underground coal mine in northern Spain is subject to violent methane (CH_4) outbursts. Vertical wells are used to extract CH_4 from coal layers to improve mine safety. Bentonite suspensions are used as drilling fluids in this degasification system. The relationship between the soil and filter cake permeabilities, the filter cake thickness, and the filtrate loss significantly affects the fluid's rheological properties. Fann mud balance, marsh funnel viscometer, and Fann 300 press filter tests have been carried out to determine the rheological properties of the bentonite suspension. A drilling fluid study was carried out for three drilling zones (across which the rheological properties of the drilling fluid vary for the reasons mentioned above): Zone 1, the lower zone, wherein drilling cuts through the coalbed; Zone 2, the upper zone, wherein drilling cuts through layers of sand; and Zone 3, an intermediate zone consisting mainly of rock. When drilling cuts through the coalbed, the release of methane, which improves the safety of underground operations, depends on the relationship between the permeability of the coal and the permeability of the filter cake of the drilling fluid. The effect of sand contamination increases the filtrate loss, and therefore also increases the permeability of the filter cake. The filtrate reducer decreases filtrate loss by recovering the permeability.

Keywords: bentonite suspension; drilling fluids; filter cake; thickness and permeability; methane degasification; vertical wells

Citation: Torno, S.; Toraño, J. Increasing Safety in an Underground Coal Mine through Degasification by Vertical Wells—Influence of the Relationship between the Permeability of Carbon and the Filter Cake of the Bentonite Suspension. *Energies* **2023**, *16*, 7223. https://doi.org/10.3390/en16217223

Academic Editor: Dameng Liu

Received: 16 September 2023
Revised: 17 October 2023
Accepted: 19 October 2023
Published: 24 October 2023

1. Introduction

The coal layer that is exploited in HVL is La Pastora, with a notable 20 to 25 m thickness, a slope of 40° to 60°, a methane (CH_4) concentration of 7 to 10 m^3/t, and a desorption rate V1 of 2. Three mining techniques are used: longwall retreat, shortwall, and sublevel caving [1].

A CH_4 emission in October 2013 resulted in the deaths of five miners. In collaboration with the University of Oviedo, HVL conducted a research project on the outburst mechanism, with the objective of predicting and controlling potential future outbursts [2]. Recent studies establish these methane predictions using mathematical formulations [3,4], neural networks [5], or three-dimensional geological seepage models [6].

One of the directions for increasing the safety and efficiency of rational integrated development of coal deposits is the advance degassing of mine fields with wells drilled from the surface [6].

Methane degasification using vertical wells was one of the CH_4 control methods [7,8] that was studied by HVL. This technique is widely used for the methane degasification, and in this way, possible outbursts are avoided [9], therefore increasing the safety of underground operations. It is important to add that once the methane has been drained,

a further step would be to use this gas as an energy resource and reduce environmental damage [5]. Studies are carried out in the mine for its future use.

Thus, advanced degassing of coal deposits using vertical wells is an effective tool for increasing the productivity and safety of coal mine. To achieve the indicated objectives, it is important that the relationship between the permeability of the carbon and the permeability of the filter cake is optimal.

Vertical wells were dug to a 550 m depth with a diamond crown drill bit using bentonite suspensions as drilling fluids [10]. In this study, the behavior of the bentonite suspension in drilling zones 1, 2, and 3 (Figure 1) was investigated: Zone 1 is the lower zone where the drilling cuts through the coalbed, zone 2 is the upper zone where the drilling cuts through layers of sand, and zone 3 is an intermediate zone consisting mainly of rock.

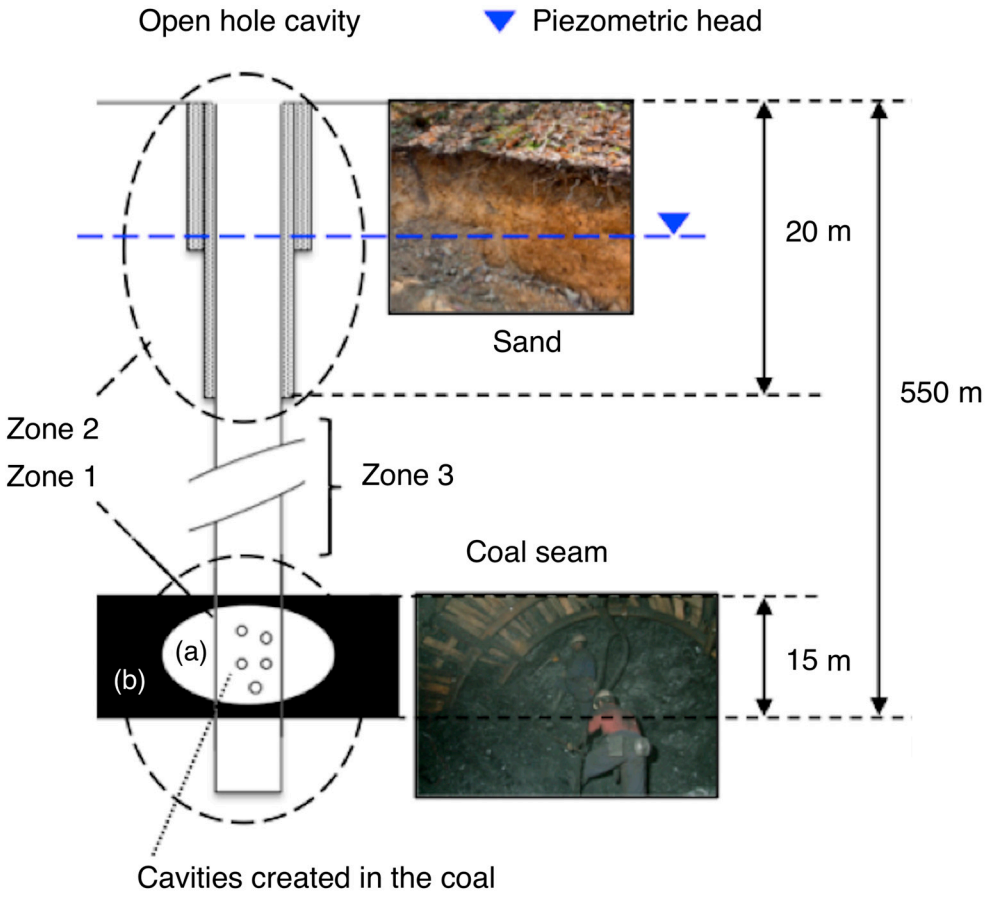

Figure 1. Vertical well and surface facilities, (**a**) annular space (**b**) coalbed.

Methane is adsorbed and stored in the matrix of the coal layer. The extraction of free CH_4 depends on the gas storage pressure [11,12] and the coal permeability [13–18]. During borehole drilling or downtime, the bentonite suspension drilling fluids form a filter cake on the sidewalls. If the permeability of the filter cake is high, some of the water in the bentonite suspension can seep into the ground [19]. If the permeability of the filter cake is low, the cake thickness increases, decreasing the diameter, and consequently the interior pressure of the borehole [20]. A filter cake with adequate permeability stabilizes the borehole sidewalls, preventing ground water from entering the borehole.

The interaction between the bentonite suspension and the soil plays a critical role in stabilizing the borehole. The slurry pressure counteracts the soil and water pressures to stabilize the borehole sidewalls. There are two models for how the confinement pressure is transferred to the drilling face (Figure 2). (a) In the filter cake model (membrane model), a thin waterproof layer is created that transfers excess suspension pressure to support

pressure. (b) In the penetration zone model, excess slurry pressure is transferred to the soil along the entire length of the penetration zone.

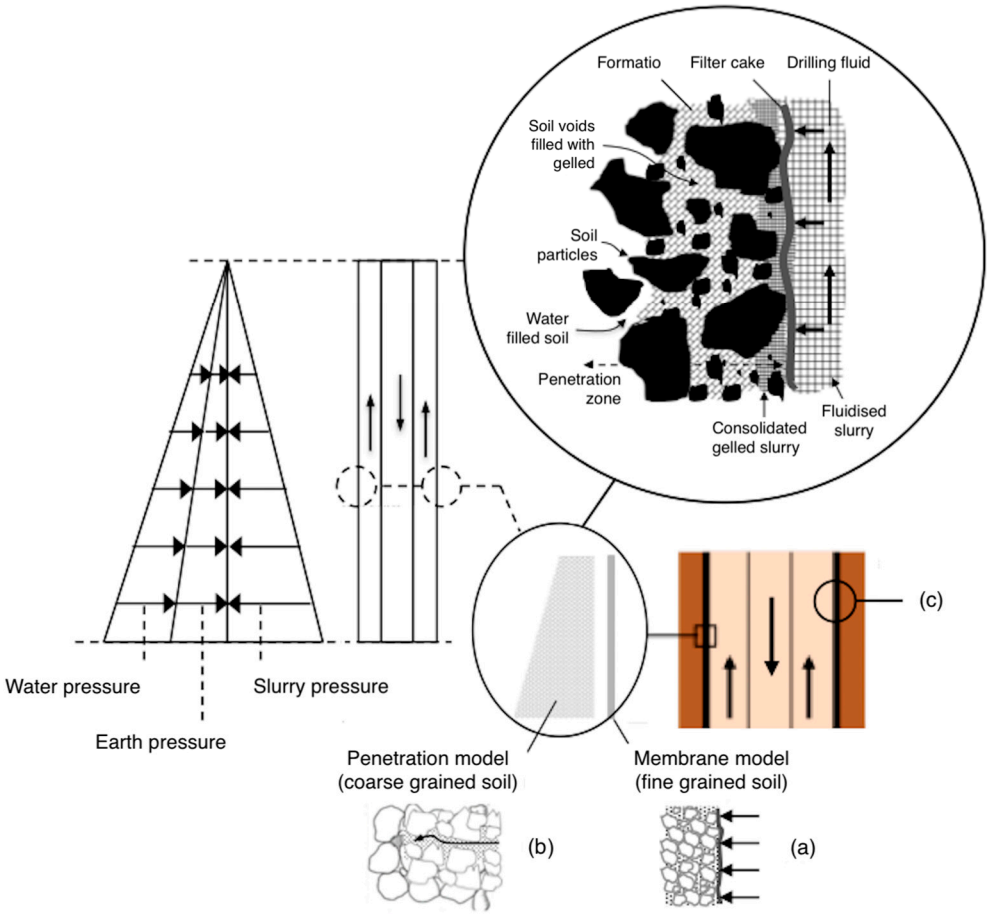

Figure 2. Formation of a filter cake (Modified after [21]) and stabilization of the borehole sidewalls, (**a**) Membrane model (**b**) Penetration model (**c**) annular space of the well.

The API normative [22–24], which is widely used and verified in the coal, gas, and oil industry, has been used for determining the rheological properties of the drilling fluid (bentonite suspension). For this, laboratory tests of the Fann mud balance, Marsh funnel viscometer, and Fann 300 press filter have been used to determine these properties. Additionally, the effect of sand contamination and the addition of filtrate reducers on three different samples of bentonite suspensions were analyzed.

The main objective of this research work is the importance of the correct implementation of vertical wells, since these can cut different types of geological materials. Of special interest is the study of the interaction between the bentonite suspension and the drilled rock because this relationship between permeabilities (bentonite suspension and the coalbed) plays a critical role in stabilizing the borehole. In this case study, special emphasis is placed on the study of the rheological properties of the bentonite suspension for the execution and durability of the vertical wells. In this way, an advanced methodology in the degasification of coalbeds before future underground coal mining work, increasing safety, can be developed.

For this reason, in this research, three areas with the following particular objectives have been analyzed:

Zone 1. (i) The relationship between the permeabilities of the coal layer and the filter cake are determined. (ii) The influence of both permeabilities on the stabilization of the borehole sidewalls is investigated for two subzones, wherein the permeabilities are different.

Zone 2. (i) The relationship between the soil and filter cake permeabilities during downtime is determined. (ii) Water formation at the top of the drilling region is investigated: this water plays a significant role in stabilizing the borehole sidewalls.

Zone 3. (i) The variation in the penetration of the suspension into the soil from filtrate loss is determined. (ii) The relationship between the annular velocity of the drilling fluid and the variation in the particle cutting slip velocity from the filter cake thickness is determined.

In all three zones, the influence of sand contamination and the action of a filtrate reducer on the bentonite suspension are examined. The results are validated using laboratory tests and measurements made in the mine.

2. Materials and Methods

2.1. Zone 1 Analysis. Coalbed

Figure 3 shows the underground mining gallery in the coal layer crossing the vertical well, and the laboratory tests on the Pastora layer coal samples. A new methodology to avoid gas loss while samples are collected by drill cutting was developed by [25]. The coal properties used in this study are shown in Table 1. The other properties of this coal are: 0.75% sulfur, 10.41% volatiles, 12.39% ash, a density of 1.45 kg/m^3, and a calorific value of 7455 Kcal/kg.

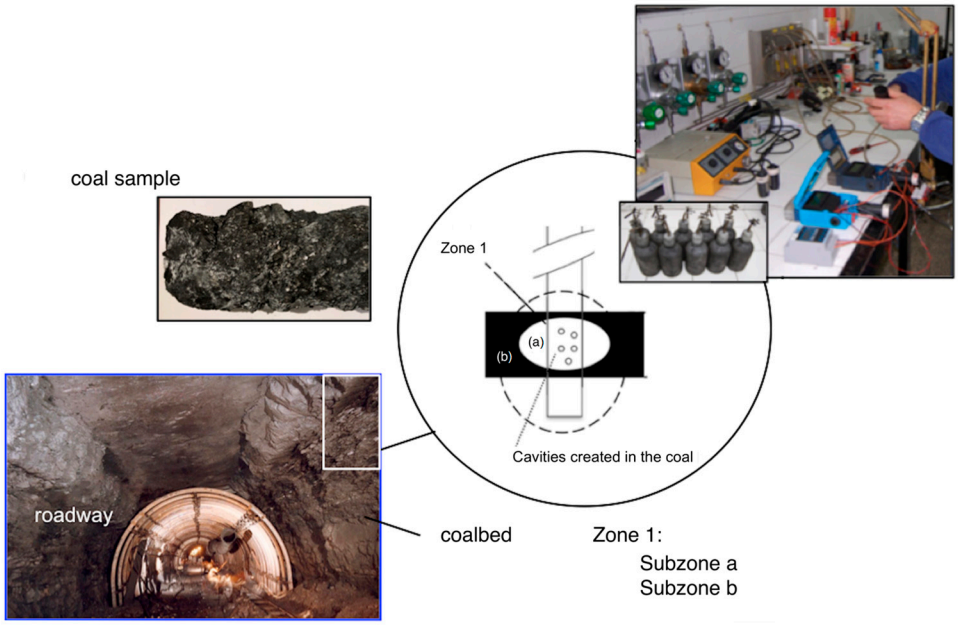

Figure 3. Mining gallery, vertical well cut, and laboratory tests.

Table 1. Average coal parameters in mined coalbed.

Q (m^3/tp)	V1 (cm^3/10 g/35 s)	Δ DCVD (a-b)	Δ GP (a-b)	Δ PI (a-b)
10–12	2–4	90	0.85	0.5

Q: CH_4 concentration in coalbed; V1: desorption rate; PI: Protodyakonov index; DCV: drill cutting volume (l/m); GP: gas pressure (MPa).

The coal permeability can be described by Equation (1) [11,26–28]:

$$K = (9.988 \times 10^{-2})/(12\ s) \cdot b^3, \quad (1)$$

where b is the space between fractures in mm, s is the length of the fracture opening in mm, and K is the permeability in cm^2. Equation (1) shows that the permeability depends on

the space and opening of the coal fracture system. However, these values vary between subzones a and b. Table 2 shows the minimum and maximum coal permeabilities (for subzones a and b), which are the average results obtained using three coal samples in each zone.

Table 2. Coal permeability.

Coal Permeability (cm^2)			
Subzone b		**Subzone a**	
Min	**Max**	**Min**	**Max**
0.06×10^{-13}	1.04×10^{-10}	1.79×10^{-10}	4.44×10^{-10}

2.2. Zone 1 Analysis. Bentonite Suspension Drilling Fluid

2.2.1. Density, Viscosity and Static Filtration

The Wyoming sodium bentonite used in this study was provided by Halliburton, and had a particle size below 70 µm [22]. Bentonite suspensions were prepared using deionized water, following the API 13A [22] and API 13I [23] guidelines for drilling fluids. The densities and viscosities of the bentonite suspensions are shown in Table 3. The pH of the suspensions was 7.00 [29,30].

Table 3. Bentonite suspension: density (Fann mud balance) and viscosity (Marsh funnel viscometer).

Bentonite Suspension Samples	Density (g/cm^3)	Viscosity (s)
Sample #1	1.021	47
Sample #2	1.029	95
Sample #3	1.034	179

After formation, the bentonite suspensions were allowed to rest in closed containers for 24 h to ensure good hydration and that the filter cake was adequately formed.

The tests on the filtrate loss and the filter cake thickness were carried out using a Fann 300 press filter (Figure 4), following the guidelines in API [24].

Figure 4a shows the relationship between the filtrate loss and the time (s) obtained from the laboratory API test with a duration of 1800 s. The repeatability and accuracy of the measurements was ensured by averaging the filtrate loss results for three tests. The first linear section reflects the instantaneous filtrate fluid loss before the formation of the filter cake, and the second linear section reflects the remaining filtrate loss that is proportional to the square root of the time.

Figure 4b shows the relationship between the filtrate loss and t (h) obtained for the laboratory API test with a duration of 24 h. The filtrate loss tended to stabilize after 8 h.

2.2.2. Filter Cake Thickness

Figure 5 shows the filter cake thickness for bentonite suspension samples #1, #2, and #3 as a function of time (h). The cake thickness increased with time, and after 8–10 h, the asymptotic thickness was between 4.9 and 6.8 mm for sample #1, between 9.7 and 11.1 mm for sample #2 and between 11.8 and 13.8 mm for sample #3.

Figure 6 shows the filter cake thickness as a function of the slurry pressure (bentonite suspensions #1, #2, and #3) for the standard API tests. In this figure, the highest value of R2 is shown by sample #2, while in the previous figure, related to the root of time, sample #1 is the one that shows a higher value of R^2.

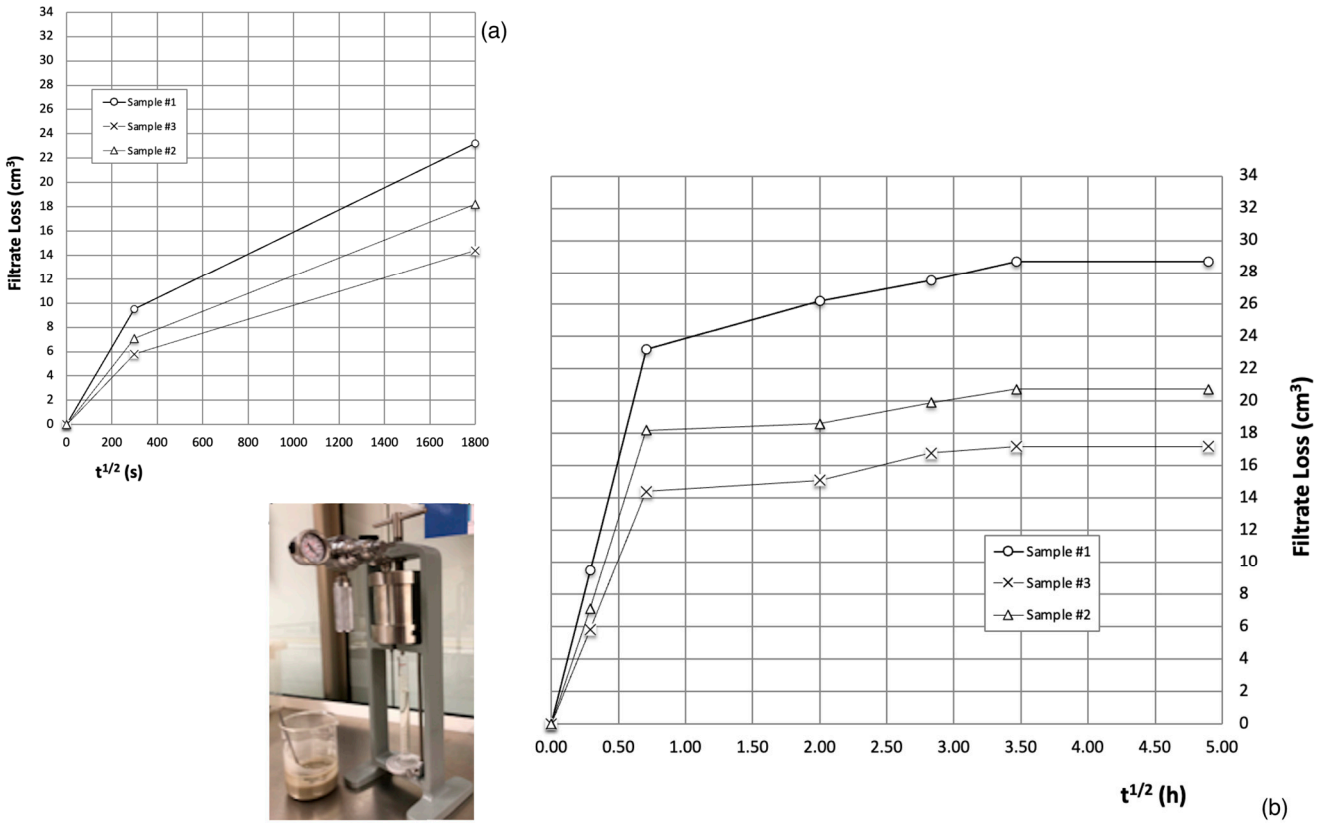

Figure 4. Relationship between filtrate loss and time (**a**) the relationship between the filtrate loss and the time (s) (**b**) the relationship between the filtrate loss and *t* (h).

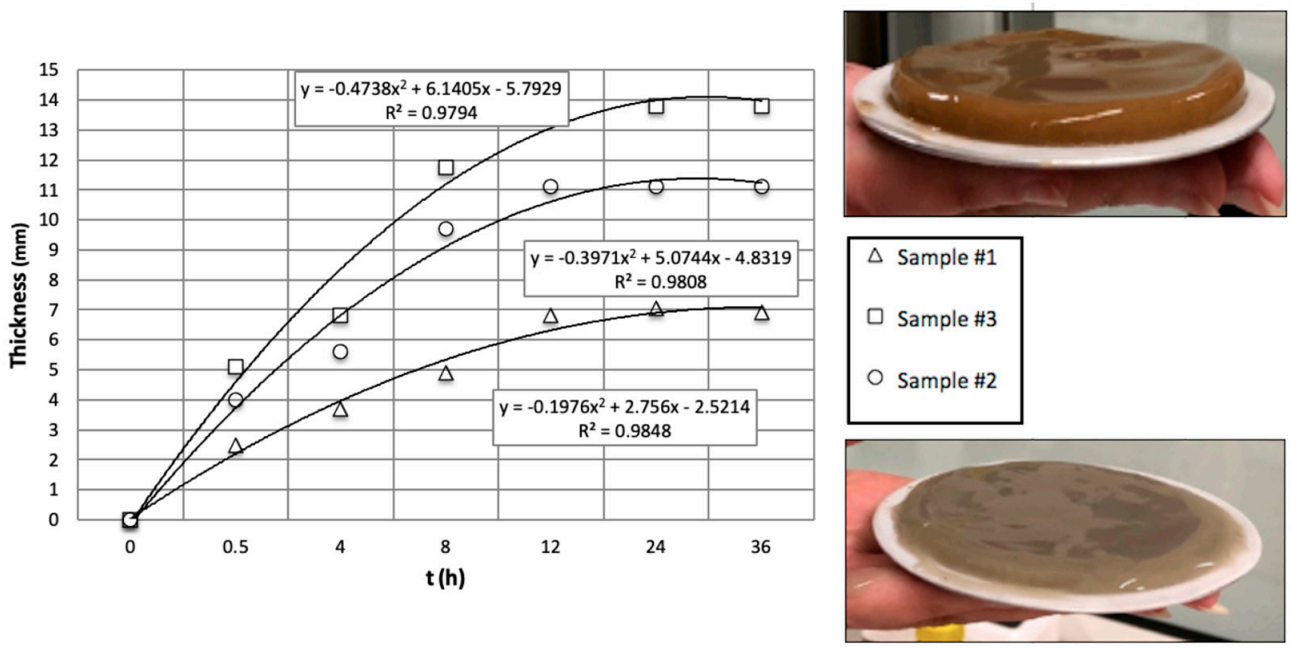

Figure 5. Filter cake thickness (test 24 h).

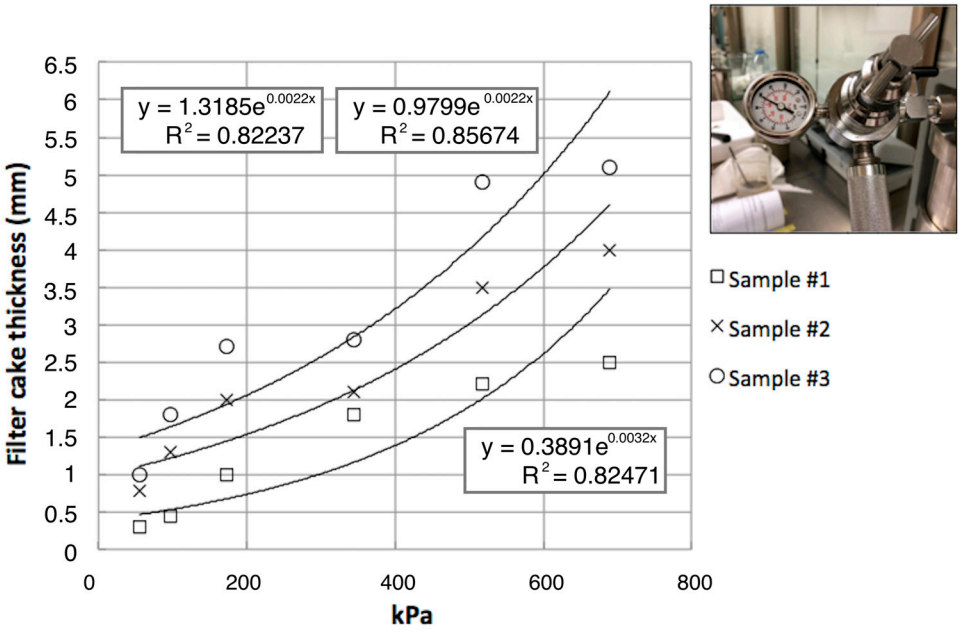

Figure 6. Filter cake thickness vs. Fluid pressure. Test 1800 s.

2.2.3. Effect of Sand Contamination by an Addition of Filtrate Reducer on Bentonite Suspension

The filtrate loss and spurt loss of bentonite suspension #1 was significantly increased by sand contamination and decreased by the addition of a filtrate reducer.

In the laboratory tests, 1.96% by volume of G-type sands with granulometry between 80 and 160 microns [30] were added to bentonite suspension sample #1. The sand content of the mineral suspension did not exceed four percent by volume.

In the tests, 0.41% of QT (QUIK-TROL, Halliburton, Houston, TX, USA) was used to reduce filtrate loss.

Table 4 shows the variations in the density and viscosity of bentonite suspension #1 upon addition of the filtrate reducer and sand at the aforementioned concentrations.

Table 4. Density and viscosity of bentonite suspension #1 with added sand and QT.

Bentonite Suspension Samples	Density (g/cm^3)	Viscosity (s)
Sample #1	1.021	47
Sample #1 with QT	1.031	119
Sample #1 with sand	1.04	60
Sample #1 with sand and QT	1.045	192

Figure 7 shows the filtrate loss under sand contamination and the action of the filtrate reducer as a function of $t^{1/2}$ for a 24-h test on bentonite suspensions #1 and #3. Sand contamination significantly increases filtrate loss (from 7.2% to 11.4%), and the filtrate reducer considerably decreases filtrate loss (from 23.1% to 24%). The filtrate loss and filter cake thickness stabilized between four and eight hours.

The filter paper with the filter cake was washed five times with a water jet from a distance of approximately 10 cm and at an incidence angle of 45°. After washing, four measurements of the filter cake thickness were taken at different points and averaged.

Figure 8 shows the effects of sand contamination and the filtrate reducer on the filter cake thickness for bentonite suspensions #1 and #3.

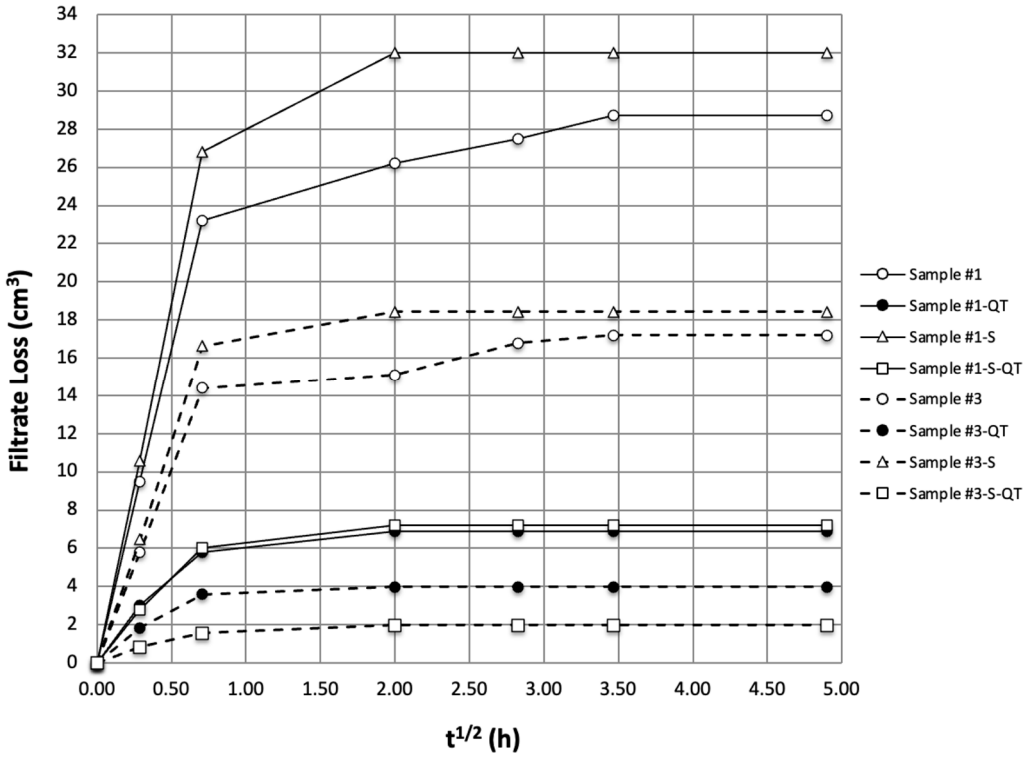

Figure 7. Filtrate loss under sand contamination and action of a filtrate reducer as a function of $t^{1/2}$.

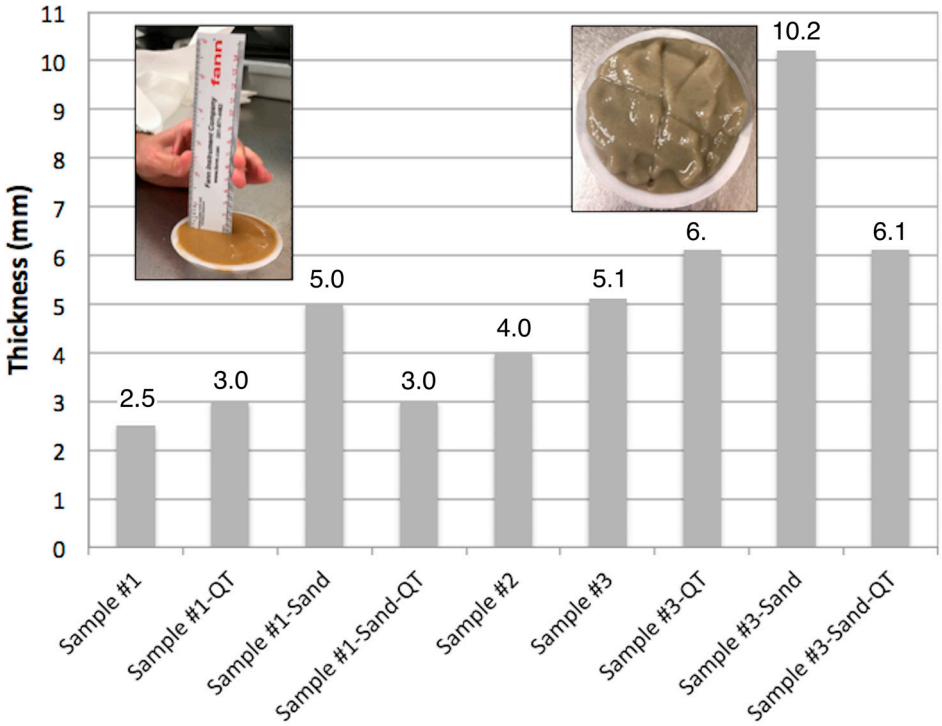

Figure 8. Effects of sand contamination and filtrate reducer on filter cake thickness.

The presence of sand (detritus) increases the slurry density, making the slurry difficult to circulate. A high sand content also results in a thick filter cake, which significantly increases filtrate loss and the filter cake permeability.

2.2.4. Permeability of Bentonite Suspension Filter Cake Compared to Coal Permeability Filter Cake Model

The mathematical equation that governs the flow of fluids through porous media is known as Darcy's Law, and can be expressed for a one-dimensional flow by Equation (2):

$$k = Q_W \cdot Q_C \cdot \mu / (2 \cdot t \cdot \Delta P \cdot A^2), \quad (2)$$

where q is the volumetric flow rate, t is the time, k is the permeability, ΔP is the pressure gradient, μ is the viscosity, h is the length of sample, Q_W is the filtrate volume, Q_C is the filter cake volume, and A is the filter cake area.

Substituting the API static filtration specifications into Equation (2) yields Equation (3):

$$k = Q_W \cdot \mu \cdot e \cdot 8.95 \times 10^{-5}, \quad (3)$$

where k is the filter cake permeability in mD, Q_W is the fluid loss in cm^3, e is the filter cake thickness in mm, and μ is the viscosity of the liquid phase of the fluid in cP.

Figure 9 shows the calculated filter cake permeabilities obtained using Equation (3) for bentonite suspensions #1, #2, and #3; bentonite suspension #1 with 3.42% sand, 0.41% QT, and both 3.42% sand and 0.41% QT. Direct laboratory measurements of the filter cake permeability by [31] are also shown.

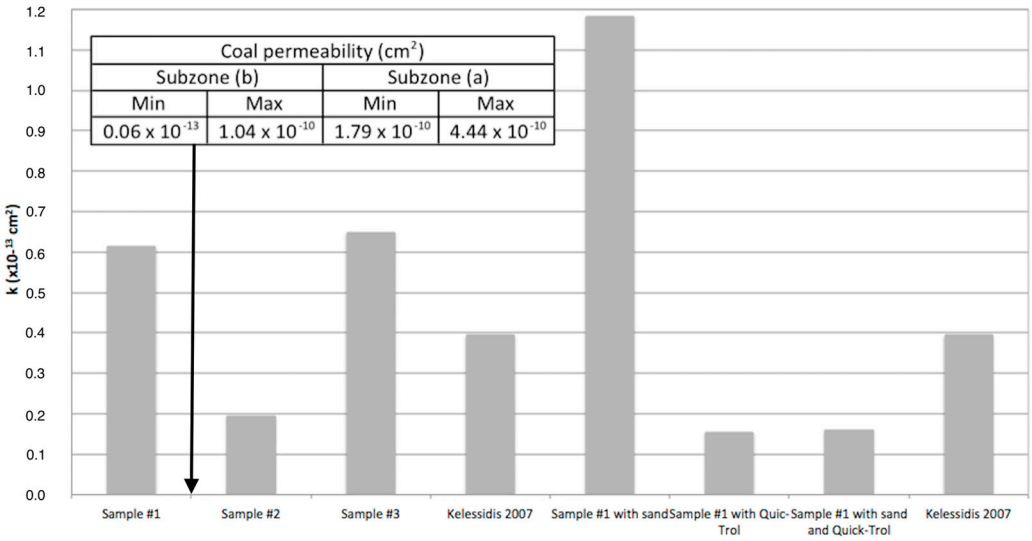

Figure 9. Filter cake permeabilities of different bentonite suspensions compared to coal permeability.

In subzone b (Figure 4), the permeability of coal (Figure 10) is below that of the bentonite suspension filter cake. Coal plays an important role in stabilizing the borehole sidewalls in subzone b. However, at maximum coal permeability, the sidewall stability is controlled by the filter cake permeability and therefore the cake thickness (Table 5).

Table 5. Shows the bentonite suspension penetration in SI units (mm).

Coal Permeability (cm^2)			
Subzone b		**Subzone a**	
Min	**Max**	**Min**	**Max**
0.06×10^{-13}	1.04×10^{-10}	1.79×10^{-10}	4.44×10^{-10}
Bentonite Suspension Penetration e (mm)			
Subzone b		**Subzone a**	
0.89	158.46	570.47	713.08

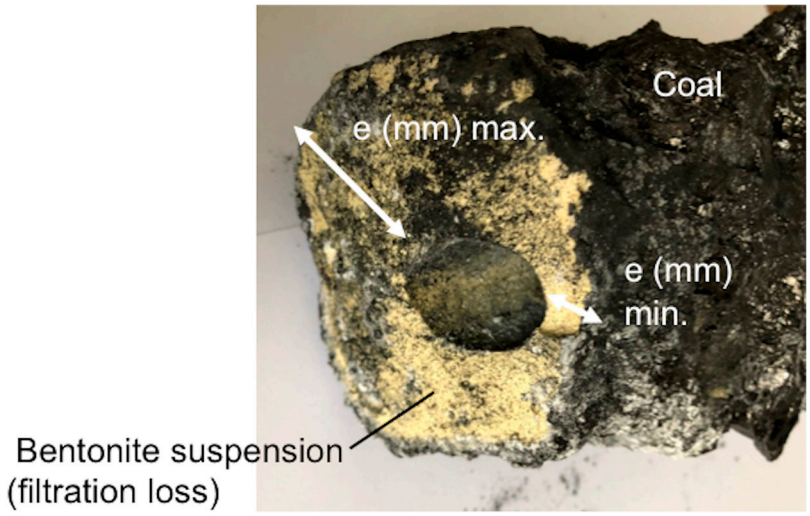

Figure 10. Coal sample from subzone b.

Penetration model:

The API static filtration specifications are given below.

- bentonite suspension volume: Q_T (API test), cm^3
- filtrate area: A (API test)
- filtrate loss volume: Q_W, cm^3
- filtrate loss per filtrate unit area: $Q_W/A = e$ cm
- filter cake volume: Q_c, cm^3
- filter cake volume per filtrate unit area: Q_C/A cm
- filtrate volume after t = 1800 s

Substituting these specifications into Equation (1) (Darcy's Law) yields Equation (4):

$$e = Q_W/A = (2{\cdot}k{\cdot}\Delta P{\cdot}t)/(\mu{\cdot}Q_C/A) = (2{\cdot}k{\cdot}\Delta P{\cdot}t\,)/(\mu{\cdot}(Q_T - Q_W)/A) = (2{\cdot}k{\cdot}\Delta P{\cdot}3600{\cdot}A)/(\mu{\cdot}(Q_T - Q_W)) \quad (4)$$

where k is the permeability (D), e (mm) is the penetration distance of the slurry in to ground (coal), ΔP at is the difference between the slurry pressure and the ground water pressure (subzone b), and μ (cp) is the viscosity of the bentonite suspension.

The bentonite suspension penetration in coal was measured for eight samples taken at the intersection of the underground mining gallery and the perforated borehole. The minimum penetration of 0.52 mm was obtained in subzone b, and the maximum penetration of 624.5 mm was obtained in subzone a (Figure 10).

2.3. Zone 2. Analysis during Downtimes

During downtime, the bleeding of the bentonite suspension may create a problematic water zone [32] at the top of the drilling region where the water and soil pressure > support pressure (subzones c and d, Figure 11). A water zone is created when the filter cake permeability falls below the soil permeability. Filtrate loss occurs at the top of the drilling region in the form of bleeding water. For equal soil and filter cake permeabilities, the filtrate loss value can be obtained using Equation (2).

The example of a borehole drilled using bentonite suspension #1, with an annular space between the hole and the drill string of 25.4 (De) cm × 14.7 (Di) cm, has been considered. The piezometric head is hp = −3 m.

Figure 12 shows the relationship between the granulometry and the permeability (in terms of the minimum, average, and maximum permeability coefficients).

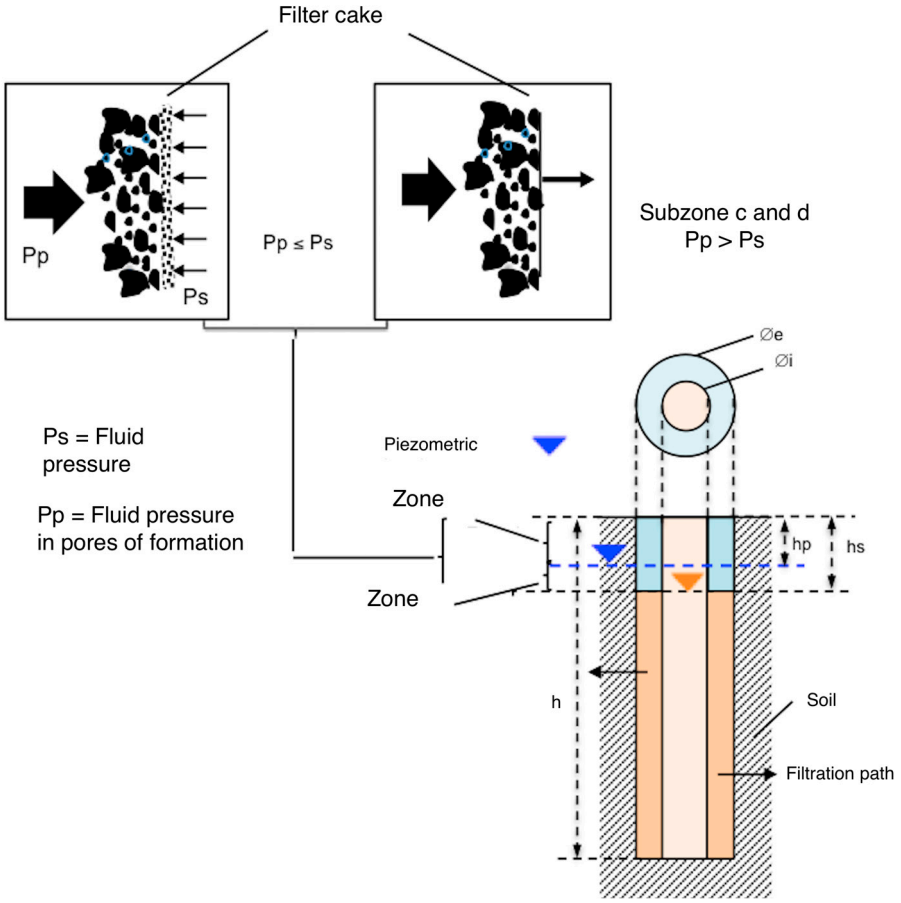

Figure 11. Filter cake formation and pressures (Zone 2).

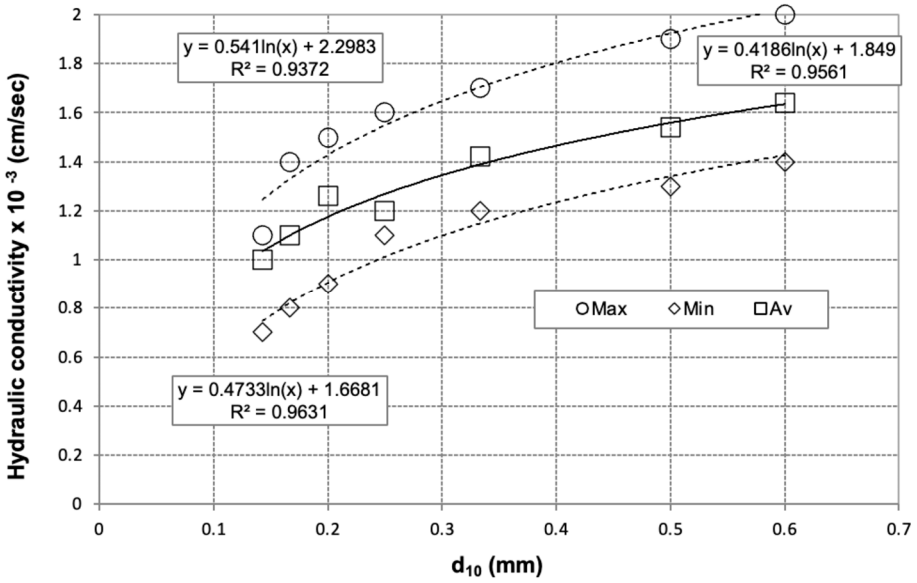

Figure 12. Granulometry vs. minimum, average and maximum permeability coefficients for G sand.

The variation in hs with d_{10} of the soil is shown in Figure 13:

- For bentonite suspension #1, the filter cake is absent in subzone c (3 m), and water can enter the soil from the borehole. The filter cake is absent in subzone d (4.5 to 6 m), and both water and soil can enter the borehole. The borehole sidewalls are unstable in both subzones.

- Sand contamination of bentonite suspension #1 increases the size of subzone d, and therefore the significance of the abovementioned problems.
- The addition of the filtrate reducer (QT) to the uncontaminated and sand-contaminated bentonite suspension #1 decreases the size of subzone c to 0.5 m. The absence of a filter cake allows water to enter the soil from the borehole and destabilizes the borehole sidewalls.

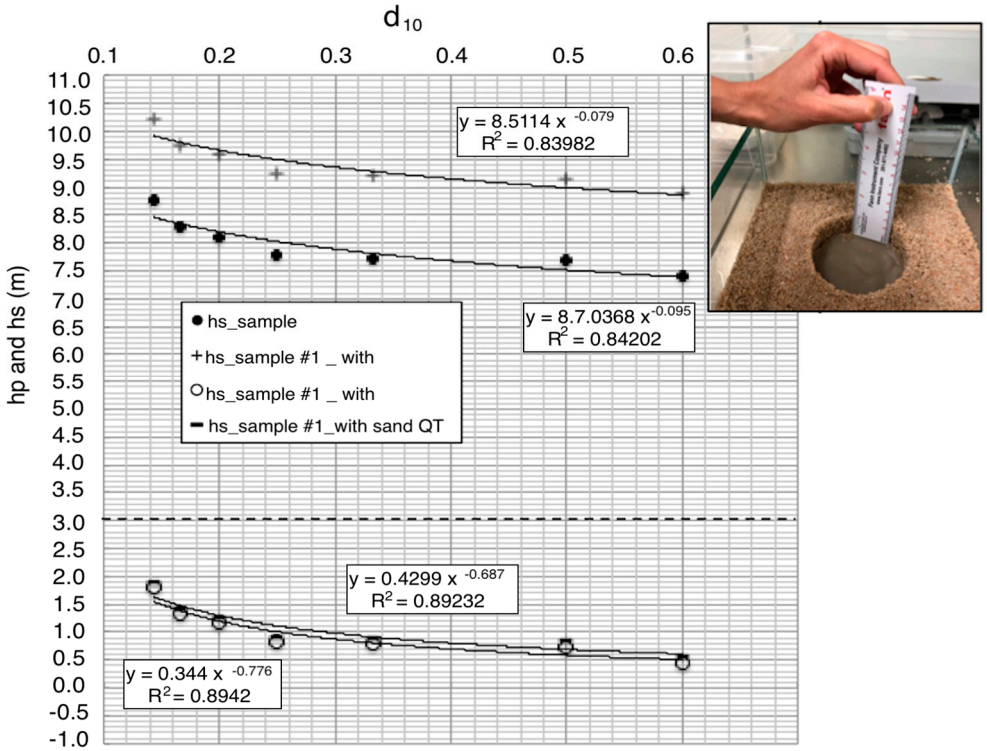

Figure 13. Variation in hp and hs for sample #1, sample #1 with sand, and sample #1 with sand and QT with d_{10}.

3. Zone 1, 2, and 3: Transport Ratio and Cutting Slip Velocity

The ground sections that are cut during drilling are displaced upwards by the drilling fluid at a rate equal to the difference between the upward fluid velocity and the downward particle slip velocity. The consistency index k and the flow behavior index n are normally used in the Chien [33] correlation [34–36] (Equation (5)) as follows:

$$v_{sl} = (2.90 \cdot d_s \cdot (\rho_s - \rho_f)^{0.667}) / (\rho_f{}^{0.333} \cdot \mu_a{}^{0.333}), \quad (5)$$

where v_{sl} is the slip velocity, d_s is the particle volume, ρ_s is the particle density, and ρ_f is the bentonite suspension density. μ_a depends on the annular space between the hole and the drill string, as well as on the coefficients n and k of the power-law model.

The transport ratio for geological drilling is calculated for the following example: the diameter and thickness of the cuttings are approximately 6.35 mm with a specific gravity of 2.58 g/cm^3; a bentonite suspension with a density of 1.078 g/cm^3 is pumped at an annular velocity of 0.609 m/s into a 25.4 cm × 14.7 cm annulus.

The following data (Table 6) were obtained in the laboratory for bentonite suspension #1 and bentonite suspension #1 with QT, with sand, and with sand and QT.

Table 6. Rheological parameters of the bentonite suspensions.

Bentonite Suspension	*d*	*n*	*k*	AVN	MV	CT	FCP
Sample #1	1.020	0.485	247.5	27.83	47	2.5	0.43604
Sample #1 with QT	1.031	0.514	288.9	37.32	119	3	0.31146
Sample #1 with sand	1.040	0.502	267.0	32.28	56	5	1.1993
Sample #1 with sand and QT	1.045	0.447	689.9	64.71	192	3	0.35442

Density *d* (g/cm^3), apparent newtonian viscosity at an annular velocity of 0.610 m/s AVN (10^{-3} Pa·s), flow behavior index *n*, consistency index *k*, marsh viscosity MV (s), cake thickness CT (mm), filter cake permeability FCP ($\times 10^{-6}$ cm^2).

Figure 14 shows the effect of contamination by sand and the effect of a filtrate reducer on the slurry annular velocity, the cutting slip velocity, the difference of both speeds, and the transport ratio, when the thickness variation in the filter cake is taken into account.

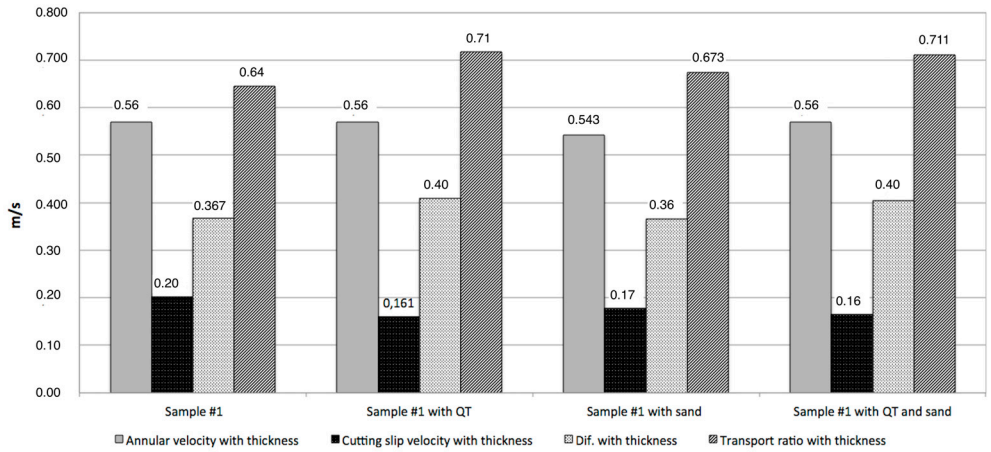

Figure 14. Parameters when the thickness variation in the filter cake is taken into account.

It can be seen that:

(a) The filtrate reducer increases the transport ratio.
(b) Contamination by sand of the slurry decreases the cutting slip velocity, and therefore increases the transport ratio.
(c) If the increase in the filter cake thickness is taken into account, (a) and (b) are fulfilled. It also decreases the transport ratio except in the case of sample #1 with filtrate reducer.

During drilling after downtimes of more than 8 h, and due to the increase in the filter cake thickness, the problems associated with the increase in the filter cake thickness become greater.

The relationship between values obtained by the models of annular velocity and cutting slip velocity, and those obtained by measuring between points one and two with plastic pipe tracers is a R^2 of 81.3.

4. Conclusions

In the analysis of the effect of drilling fluid on degasification by vertical wells, three zones with different requirements for the properties of the drilling fluid were considered.

Zone 1: In the filter cake model, coal permeability is lower than the filter cake permeability of the bentonite suspension. Coal is important in the stabilization of the borehole sidewalls in that zone. However, there are maximum values of coal permeability where the fundamental aspect is the filter cake permeability, and therefore its thickness. Penetration values of the bentonite suspension (penetration model) are at a minimum in subzone b (0.89 mm) and at a maximum in subzone a (713 mm).

Zone 2: For bentonite suspension sample #1, the borehole sidewalls are unstable in both subzones c and d. For bentonite suspension sample #1 contaminated with sand, the above-mentioned problems are more important due to the increase in subzone d.

When a filtrate reducer (QT) is added to bentonite suspension sample #1 and to sample #1 contaminated with sand, subzone c decreases to values of 0.5 m. There is no filter cake, there is possible water entry from the borehole to the soil, and the borehole sidewalls are unstable.

Zone 3. It can be seen that the filtrate reducer increases the transport ratio. Contamination by sand of the slurry decreases the cutting slip velocity, and therefore increases the transport ratio. If the increase in the filter cake thickness is taken into account, the transport ratio decreases. During drilling after downtimes of more than 8 h, and due to the increase in the filter cake thickness, the problems become greater.

The next step would be to determine predictive models to increase the efficiency of the vertical wells of the methane degasification, as well as seek to use this gas for energy and reduce environmental damage.

Author Contributions: Conceptualization, J.T. and S.T.; methodology, J.T.; software, S.T.; validation, S.T.; formal analysis, J.T.; investigation, S.T. and J.T.; resources, S.T.; data curation, S.T. and J.T.; writing—original draft preparation, J.T.; writing—review and editing, S.T.; visualization, S.T.; supervision, S.T. and J.T.; project administration, S.T. and J.T.; funding acquisition, J.T. All authors have read and agreed to the published version of the manuscript.

Funding: This research was funded by Hullera Vasco Leonesa S.A. Company, (Vice-Rectorate for Research: 0039/001).

Data Availability Statement: The data presented in this study are available on request from the corresponding author. The data is not publicly available due to the fact that the data is judicially required by the incident which occurred at the mine.

Acknowledgments: This research has been carried out by the Mining and Civil Works Research Group of University of Oviedo (Vice-Rectorate for Research: 0039/001) in collaboration with Hullera Vasco Leonesa S.A. Company. We would like to thank Hullera Vasco Leonesa S.A. Mining Company for the access to their underground mines and for financing this study.

Conflicts of Interest: The authors declare no conflict of interest. The funders had no role in the design of the study; in the collection, analyses, or interpretation of data; in the writing of the manuscript; or in the decision to publish the results.

References

1. Toraño, J.; Torno, S.; Menendez, M.; Gent, M.; Velasco, J. Models of methane behaviour in auxiliary ventilation of underground coal mining. *Int. J. Coal Geol.* **2009**, *80*, 35–43. [CrossRef]
2. Toraño, J.; Torno, S.; Alvarez, E.; Riesgo, P. Application of outburst risk indices in the underground coal mines by sublevel caving. *Int. J. Rock Mech. Min. Sci.* **2012**, *50*, 94–101. [CrossRef]
3. Zhang, X.; Zhu, T.; Yi, N.; Yuan, B.; Li, C.; Ye, Z.; Zhu, Z.; Zhang, X. Study on Characteristics and Model Prediction of Methane Emissions in Coal Mines: A Case Study of Shanxi Province, China. *Atmosphere* **2023**, *14*, 1422. [CrossRef]
4. Bosikov, I.I.; Martyushev, N.V.; Klyuev, R.V.; Savchenko, I.A.; Kukartsev, V.V.; Kukartsev, V.A.; Tynchenko, Y.A. Modeling and Complex Analysis of the Topology Parameters of Ventilation Networks When Ensuring Fire Safety While Developing Coal and Gas Deposits. *Fire* **2023**, *6*, 95. [CrossRef]
5. Tutak, M.; Brodny, J. Forecasting Methane Emissions from Hard Coal Mines Including the Methane Drainage Process. *Energies* **2019**, *12*, 3840. [CrossRef]
6. Krassakis, P.; Pyrgaki, K.; Gemeni, V.; Roumpos, C.; Louloudis, G.; Koukouzas, N. GIS-Based Subsurface Analysis and 3D Geological Modeling as a Tool for Combined Conventional Mining and In-Situ Coal Conversion: The Case of Kardia Lignite Mine, Western Greece. *Mining* **2022**, *2*, 297–314. [CrossRef]
7. Mutmansky, J.M.; Thakur, P.C. *Guidebook on Coalbed Methane Drainage for Underground Coal Mine*; USEPA No. CX824467-01-0; Pennsylvania State University: State College, PA, USA, 1999.
8. Xu, T.; Tang, C.A.; Yang, T.H.; Zhu, W.C.; Liu, J. Numerical investigation of coal and gas outbursts in underground collieries. *Int. J. Rock Mech. Min. Sci.* **2006**, *43*, 905–919. [CrossRef]

9. Karacan, C.O. Predicting methane emissions and developing reduction strategies for a Central Appalachian Basin, USA, longwall mine through analysis and modeling of geology and degasification system performance. *Int. J. Coal Geol.* **2023**, *270*, 104234. [CrossRef]
10. Li, D. A new technology for the drilling of long boreholes for gas drainage in a soft coal seam. *J. Petrol. Sci. Eng.* **2016**, *137*, 107–112. [CrossRef]
11. Pan, Z.; Connell, L.D.; Camilleri, M. Laboratory characterisation of coal reservoir permeability for primary and enhanced coalbed methane recovery. *Int. J. Coal Geol.* **2010**, *82*, 252–261. [CrossRef]
12. Lu, M.; Connell, L. A dual-porosity model for gas reservoir flow incorporating adsorption behaviour-part I. Theoretical development and asymptotic analyses. *Transp. Porous Media* **2007**, *68*, 153–173. [CrossRef]
13. Somerton, W.H.; Söylemezoglu, I.M.; Dudley, R.C. Effect of stress on permeability of coal. *Int. J. Rock Mech. Min. Sci. Geomech. Abstr.* **1975**, *12*, 129–145. [CrossRef]
14. Reid, G.W.; Towler, B.F.; Harris, H.G. Simulation and Economics of Coalbed Methane Production in Power River Basin. In Proceedings of the SPE Rocky Mountain Regional Meeting, Casper, WY, USA, 18–21 May 1992; Society of Petroleum Engineers: Dallas, TX, USA, 1992.
15. Sherwood, J.D.; Meeten, G.H. The filtration properties of compressible mud filtercakes. *J. Petrol. Sci. Eng.* **1987**, *18*, 73–81. [CrossRef]
16. Sparks, D.P.; McLendon, T.H.; Saulsberry, J.L.; Lambert, S.W. The Effects of Stress on Coalbed Reservoir Performance. In Proceedings of the SPE Annual Technical Conference and Exhibition, Dallas, TX, USA, 22–25 October 1995; Society of Petroleum Engineers: Dallas, TX, USA, 1995.
17. Palmer, I. Permeability changes in coal: Analytical modeling. *Int. J. Coal Geol.* **2009**, *77*, 119–126. [CrossRef]
18. Palmer, I. Coalbed methane completions: A world view. *Int. J. Coal Geol.* **2010**, *82*, 184–195. [CrossRef]
19. Chapuis, R.P. Estimating the in situ porosity of sandy soils sampled in boreholes. *Eng. Geol.* **2012**, *141–142*, 57–64. [CrossRef]
20. Chilingarian, G.V.; Vrabutr, P. *Drilling and Drilling Fluids*; Developments in Petroleum Science; U.S. Department of Energy Office of Scientific and Technical Information: Oak Ridge, TN, USA, 1983; p. 11.
21. Khodja, M. Drilling Fluid: Performance Study and Environmental Considerations. Ph.D. Thesis, L'Institut National Polytechnique de Toulouse, Toulouse, France, 2008. (In French).
22. API (American Petroleum Institute Specifications). *Specification for Drilling Fluid Materials*; API 13A; API: Washington, DC, USA, 1993.
23. API (American Petroleum Institute Specifications). *Recommended Practice Standard Procedure for Laboratory Testing Drilling Fluids*; API 13I; API: Washington, DC, USA, 2000.
24. API (American Petroleum Institute Specifications). *Recommended Practice Standard Procedure for Field Testing Water-Based Drilling FIuids*; API RP 13B-1; API: Washington, DC, USA, 2019.
25. Szlząk, N.; Korzec, M.; Piergies, K. The Determination of the Methane Content of Coal Seams Based on Drill Cutting and Core Samples from Coal Mine Roadway. *Energies* **2022**, *15*, 178. [CrossRef]
26. Gray, I. Reservoir Engineering in Coal Seams, Part 1-The Physical Process of Gas Storage and Movement in Coal Seams. *SPE Reserv. Eng.* **1987**, *2*, 28–34. [CrossRef]
27. Wang, S.; Elsworth, D.; Liu, J. Permeability evolution during progressive deformation of intact coal and implications for instability in underground coal seams. *Int. J. Rock Mech. Min. Sci.* **2013**, *58*, 34–45. [CrossRef]
28. Zhou, H.; Gao, J.; Han, K.; Cheng, Y. Permeability enhancements of borehole outburst cavitation in outburst-prone coal seams. *Int. J. Rock Mech. Min. Sci.* **2018**, *111*, 12–20. [CrossRef]
29. Alderman, N.; Ram, B.D.; Hughes, T.; Maitland, G. The rheological properties of water-based drilling fluids—Effect of bentonite chemistry. *Spec. Chem Prod Mark. Appl.* **1989**, *9*, 314–326.
30. Kumar, R.; Kumar, V.; Rajak, D.K.; Guria, C. An improved estimation of shear rate using rotating coaxial-cylinder Fann viscometer: A rheological study of bentonite and fly ash suspensions. *Int. J. Miner. Process.* **2014**, *126*, 18–19. [CrossRef]
31. *ISO 3310-1:2016*; Test Sieves. Technical Requirements and Testing. Part 1: Test Sieves of Metal Wire Cloth. ISO (International Organization for Standardization): Geneva, Switzerland, 2016.
32. Baptiste, N.; Chapuis, R.P. What maximum permeability can be measured with a monitoring well? *Eng. Geol.* **2015**, *184*, 111–118. [CrossRef]
33. Chien, S.F. Annular Velocity for Rotary Drilling Operations. *J. Rock Mech. Min. Sci. Geomech. Abstr.* **1972**, *9*, 403–416. [CrossRef]
34. Kelessidis, V.C.; Tsamantaki, C.; Pasadakis, N.; Repouskou, E.; Hamilaki, E. Permeability, porosity and surface characteristics of filter cakes from water–bentonite suspensions. *WIT Trans. Eng. Sci.* **2007**, *56*, 173–182.
35. Moore, P.L. *Drilling Practices Manual*, 1st ed.; Petroleum Publishing Co.: Tulsa, OK, USA, 1974.
36. Bourgoyne, A.; Miliheim, K.; Chenevert, M.; Young, K.S. *Applied Drilling Engineering*, 2nd ed.; Society of Petroleum Engineers: Richardson, TX, USA, 1986.